Strong-flow gyrokinetic simulations with a unified treatment of all length scales

A.Y. Sharma[1], B.F. McMillan[1], J. Dominski[2]

[1] *Centre for Fusion, Space and Astrophysics, University of Warwick, Coventry, UK*

[2] *Princeton Plasma Physics Laboratory, Princeton, US*

Introduction

The gyrokinetic ordering parameter was originally[1]

$$\varepsilon \sim \omega\Omega^{-1} \sim k_{\|}\rho_{\mathrm{t}} \sim \rho_{\mathrm{t}}L_{\mathrm{B}}^{-1} \sim q\phi T^{-1} \ll 1, k_{\perp}\rho_{\mathrm{t}} \sim 1, \tag{1}$$

where ω is the characteristic fluctuation frequency, Ω is the gyrofrequency, $k_{\|}$ is the characteristic fluctuation parallel wavenumber, ρ_{t} is the thermal gyroradius, L_{B} is the magnetic field length scale, q is the particle charge, ϕ is the electrostatic potential, T is the temperature and $k_{\perp}$ is the characteristic fluctuation perpendicular wavenumber. Ordering (1) can be generalised[2] to give a weak-flow gyrokinetic ordering parameter,

$$\varepsilon \sim \omega\Omega^{-1} \sim k_{\|}\rho_{\mathrm{t}} \sim \rho_{\mathrm{t}}L_{\mathrm{B}}^{-1} \sim uv_{\mathrm{t}}^{-1} \ll 1, \tag{2}$$

where u is the E×B drift speed associated with ϕ and v_{t} is the thermal particle speed. Ordering (2) cannot be applied to all modern tokamak plasmas in general due to the presence of large flows. A further generalisation[3] gives a strong-flow gyrokinetic ordering,

$$\varepsilon \sim \omega\Omega^{-1} \sim k_{\|}\rho_{\mathrm{t}} \sim \rho_{\mathrm{t}}L_{\mathrm{B}}^{-1} \sim u'\Omega^{-1} \ll 1, \tag{3}$$

where u' is the magnitude of the spatial derivatives of the E×B drift velocity associated with ϕ. Using Ordering (3), we present the discretisation of our manifestly conservative Vlasov-Poisson system that is obtained directly from our gyrocentre Lagrangian[4].

Lagrangian

Our gyrocentre Lagrangian for electrostatic potential perturbations in slab magnetic geometry up to first order is

$$\Gamma = \left[\boldsymbol{A}(\boldsymbol{R}) + v_{\|}\hat{\boldsymbol{b}} + \boldsymbol{u}\right] \cdot \mathrm{d}\boldsymbol{R} + \mu\,\mathrm{d}\theta - \left(\tfrac{1}{2}v_{\|}^2 + \mu B + \tfrac{1}{2}\boldsymbol{u}^2 + \langle\phi\rangle\right)\mathrm{d}t, \tag{4}$$

where we use units such that $m = q = T = 1$, m is the particle mass, T is the temperature, q is the particle charge, $\boldsymbol{A}$ is the magnetic vector potential, $\boldsymbol{R}$ is the gyrocentre position, $\hat{\boldsymbol{b}}$ is the magnetic field unit vector, $\boldsymbol{u} = B^{-1}\hat{\boldsymbol{b}} \times \boldsymbol{\nabla}\langle\phi\rangle$, $\langle\psi\rangle(\boldsymbol{R},\mu,t) = (2\pi)^{-1}\int \mathrm{d}\theta\mathrm{d}^3r\,\delta(\boldsymbol{R}+\boldsymbol{\rho}-\boldsymbol{r})\psi(\boldsymbol{r},t)$

for any function ψ, μ is the conserved magnetic moment, t is time, θ is the gyroangle, $\boldsymbol{r}$ is the particle position and $\boldsymbol{\rho}$ is the gyroradius.

This Lagrangian (4) does not contain any $\mathcal{O}(\varepsilon)$ terms, as these have all been Lie-transformed to higher order.

Vlasov-Poisson system

The Vlasov-Poisson system obtained from our Lagrangian (4) is then

$$\begin{aligned} &F_{,t} + \dot{R}_i F_{,i} = 0, \\ &\dot{\boldsymbol{R}} = \boldsymbol{u} + B_{\parallel}^{*-1} \hat{\boldsymbol{b}} \times \dot{\boldsymbol{u}}_1, \\ &\dot{v}_{\parallel} = 0, \\ &0 = \int \mathrm{d}^6 Z \delta(\boldsymbol{R} + \boldsymbol{\rho} - \boldsymbol{r}) [B_{\parallel}^{*} F + B^{-1} \hat{\boldsymbol{b}} \cdot \boldsymbol{\nabla} \times F(\hat{\boldsymbol{b}} \times \dot{\boldsymbol{u}}_1)], \end{aligned} \tag{5}$$

where F is the distribution function that transforms as a scalar, $F_{,\theta} = 0$, $\Psi_{,\alpha} = \partial_\alpha \Psi$ for any quantity Ψ and any coordinate α, $i \in \{1,2,3\}$,

$$B_{\parallel}^{*} = \hat{\boldsymbol{b}} \cdot (\boldsymbol{B} + \boldsymbol{\nabla} \times \boldsymbol{u}), \tag{6}$$

$\dot{\boldsymbol{u}}_1 = (\partial_t + \boldsymbol{u} \cdot \boldsymbol{\nabla})\boldsymbol{u}$ and $Z = (\boldsymbol{R}, \mu, v_{\parallel}, \theta)$.

Numerical Scheme

The second term in $\dot{\boldsymbol{R}}$ (5) and the second term in the square brackets in our Poisson equation (5) contain a partial time derivative of the potential-dependent flow velocity. We use that these terms are one order smaller in ε than their neighbouring terms in order to facilitate the numerical solution of our Vlasov-Poisson system (5). We choose to solve our Vlasov-Poisson equations (5) using a δf particle-in-cell (PIC) method, as in [5]. That is to say, we use Monte Carlo markers to represent distribution function quanta that are evolved according to consistent fields, whilst employing the splitting

$$F = F_0 + \delta F,$$

where we choose the equilibrium part $F_0 = n_0 (2\pi T)^{-\frac{3}{2}} e^{-\frac{1}{2}v^2/T}$ to be Maxwellian, $n_0(\boldsymbol{R})$ is the background density, $T(\boldsymbol{R})$ is the temperature, v is the particle velocity and the fluctuating part δF is discretised as follows. We define

$$\delta F = N_{\mathrm{p}} N^{-1} \sum_{n=1}^{N} 2\pi B_{\parallel}^{*-1} w_n(t) \delta(\boldsymbol{R} - \boldsymbol{R}_n(t)) \delta(\mu - \mu_n(t)) \delta(v_{\parallel} - v_{\parallel n}(t)),$$

where N_{p} is the number of particles, N is the number of markers,

$$w_n = \delta F_n V_{\mathrm{p}n} \tag{7}$$

is the marker *weight*, δF_n is the average value of δF in the marker phase space volume

$$V_{\mathrm{p}n} = \mathrm{d}^6 z_n \mathrm{d}N_n^{-1}, \tag{8}$$

$\mathrm{d}^6 z_n = B_{\parallel}^* \mathrm{d}^3 R \mathrm{d}\mu \mathrm{d}v_{\parallel} \mathrm{d}\theta$ is an infinitesimal,

$$\mathrm{d}N_n = N N_{\mathrm{p}}^{-1} f_{\mathrm{m}}(\boldsymbol{R}, v_{\perp}, v_{\parallel}) \mathrm{d}^3 R v_{\perp} \mathrm{d}v_{\perp} \mathrm{d}v_{\parallel} \mathrm{d}\theta$$

is the number of markers in $\mathrm{d}^6 z_n$ and f_{m} is an arbitrary probability density function that transforms as a scalar density. Since our $B_{\parallel}^*$ is potential-dependent (6), we initially use $B_{\parallel}^* = B$ when computing $V_{\mathrm{p}n}$ (8). However, upon computing the potential, we may compute $B_{\parallel}^*$ correctly (6), and thus correct V_{pn}. Additionally, we may choose to keep ϕ constant when correcting V_{pn}: in order to do this, we keep w_n constant and adjust δF_n using Equation 7. The only consequence of doing this is that initialisation with a particular distribution function is hindered. We may initially neglect the second term in the square brackets in our Poisson equation (5). We may approximate $\dot{\boldsymbol{u}}_1$ with a forward difference by taking a time step using $\dot{\boldsymbol{R}} = \boldsymbol{u}$.

Slab results

In the case of a weak-flow, each interacting vortex pulls the other around its centre, resulting in propagation. In the case of a strong-flow, there is a shift in the rotation frequency of the vortices that depends on the sign of the vorticity.

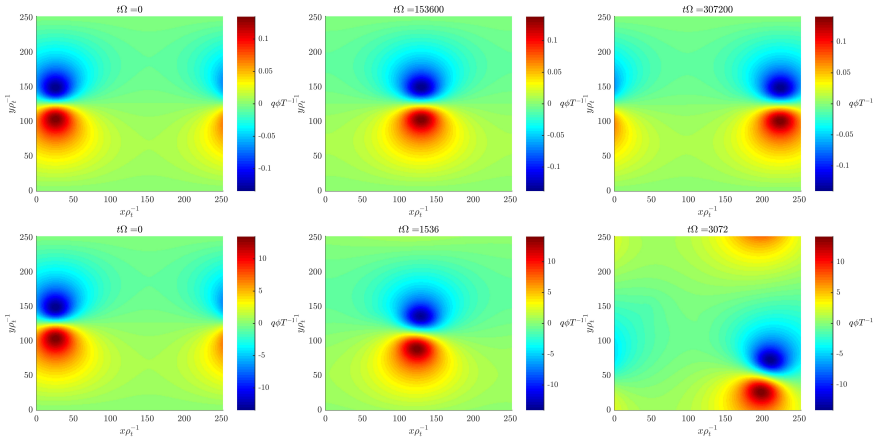

Fig. 3. Comparison of weak- (top) and strong- (bottom) flow blob propagation, where we have used periodic boundary conditions.

Stand-alone Poisson solver

We have developed a stand-alone Poisson solver with the following features: arbitrary-wavelength perturbations; cubic B-spline finite-element discretisation; slab and cylindrical geometries; background density and temperature gradients; MPI parallelisation; Fortran source code; based on the solver from the ORB5 code [6]. The following features are planned: extension to three dimensions; field-aligned geometry; nonlinear solution via a multigrid approach.

Solution of our Poisson equation

Due to the presence of ϕ in the symplectic part of our Lagrangian (4), $\dot{\boldsymbol{u}}_1$ (5) is present in our Poisson equation (5). Formally, we may solve our Vlasov-Poisson system by writing our system Lagrangian L_s is terms of our particle Lagrangian L_p as

$$L_\mathrm{s} = \int \mathrm{d}ZFL_\mathrm{p}[Z,\dot{Z},\phi(Z,\dot{Z})],$$

where species and temporal subscripts have been suppressed. Whilst a formal solution for $\dot{Z}$ and ϕ exists, it is computationally intractable due to the dependence of ϕ on $\dot{Z}$ (5). We may use that the second term in the square brackets in our Poisson equation (5) is one order smaller in ε than the first term, and perform an iterative solution of our Vlasov-Poisson system (5).

Conclusions and future work

A strong-flow gyrokinetic theory with a unified treatment of all length scales has been numerically implemented. Our Vlasov-Poisson system (5) is manifestly conservative, as it is obtained as a whole, directly from our Lagrangian (4). We use an iterative numerical solution of our Vlasov-Poisson system (5). We see strong-flow symmetry-breaking that depends on the sign of $B^*_\parallel$ (6). Code verification has been performed with basic slab instabilities. An arbitrary-wavelength, stand-alone Poisson solver has been developed based on the ORB5 code [6]. The manifest conservation of our Vlasov-Poisson system (5) is preserved with our finite-element discretisation.

Centrifugal and drift instability simulations are to be performed. An ultimate goal would be a general magnetic geometry, electromagnetic numerical implementation.

References

[1] T S Hahm. *Phys. Fluids*, 31(9):2670–2673, 1988.

[2] A. M. Dimits, L. L. LoDestro, and D. H. E. Dubin. *Phys. Fluids B*, 4(1):274, 1992.

[3] Andris M. Dimits. *Phys. Plasmas*, 17(5):055901, 2010.

[4] B. F. McMillan and A. Sharma. *Physics of Plasmas*, 23(9):092504, 2016.

[5] S. Jolliet, A. Bottino, P. Angelino, R. Hatzky, T. M. Tran, B. F. McMillan, O. Sauter, K. Appert, Y. Idomura, and L. Villard. *Comput. Phys. Commun.*, 177(5):409–425, 2007.

[6] J. Dominski, B. F. McMillan, S. Brunner, G. Merlo, T.-M. Tran, and L. Villard. *Physics of Plasmas*, 24(2):022308, 2017.